J. Phys.: Condens. Matter **20** (2008) 015224 (5pp) doi:10.1088/0953-8984/20/01/015224

Order–disorder character of $PbTiO_3$

Young-Han Shin[1], Jong-Yeog Son[1], Byeong-Joo Lee[1], Ilya Grinberg[2] and Andrew M Rappe[2]

[1] Department of Materials Science and Engineering, Pohang University of Science and Technology, Pohang 790-784, Republic of Korea
[2] Makineni Theoretical Laboratories, Department of Chemistry, University of Pennsylvania, Philadelphia, PA 19104-6323, USA

E-mail: sonjyson@postech.ac.kr

Received 6 July 2007, in final form 15 November 2007
Published 12 December 2007
Online at stacks.iop.org/JPhysCM/20/015224

Abstract

We report the displacive and order–disorder characters of $PbTiO_3$ analyzed using a classical atomic model which was developed under the inverse relation between the bond length and the bond valence. The ferroelectric phase changes to the paraelectric phase around 700 K, and the histograms of Ti–O and Pb–O bond lengths have three peaks which become a single peak above the phase transition temperature. The order–disorder character of this material was clearly shown by analyzing the ion displacement magnitudes.

(Some figures in this article are in colour only in the electronic version)

Ferroelectricity in perovskites has been widely investigated due to applications like nonvolatile random access memory [1–3]. Comes *et al* used x-ray scattering to study the structural disorder of $BaTiO_3$ and $KNbO_3$ [4]. Starting from the work of Comes *et al* the *n*-site model was developed and studied with first-principles calculations [5, 6]. $PbTiO_3$ has a simple structural phase transition compared to the other perovskites such as $BaTiO_3$. While $PbTiO_3$ has been believed to be a typical displacive ferroelectric, some experimental evidence reveals an order–disorder behavior in this material [7–9]. The evidence suggests that the Pb ions are disordered over six sites along the cubic principal axes. Unfortunately, despite the evidence that supports the notion of an order–disorder behavior in $PbTiO_3$, there is difficulty in interpreting experimental results.

First-principles calculations have been used for studying and understanding ferroelectrics. Differences in the ferroelectric phase transition (including the effect of tetragonal strain) between $BaTiO_3$ and $PbTiO_3$ were studied with the first-principles calculations [10], and a few atomic potential models based on the density functional theory have been developed [11–15]. In the case of $BaTiO_3$, the order–disorder and displacive characters during the phase transitions were examined with an effective Hamiltonian approach specified by the first-principles pseudopotential calculations [16, 17]. In order to study the displacive and order–disorder characters of $PbTiO_3$, we use a classical model potential based on the inverse relation between the bond valence and the bond length. The parameters of this potential model were fit to the reference structures obtained from first-principles calculations developed for ionic systems [13].

The total interatomic potential of the bond-valence model is given by:

$$E_{\mathrm{bv}} = E_{\mathrm{c}} + E_{\mathrm{r}} + E_{\mathrm{b}} + E_{\mathrm{a}}, \tag{1}$$

where E_{c} is a Coulombic potential, E_{r} is a short-range repulsive potential, E_{b} is a potential for the bond-valence relation, and E_{a} is an angle potential which is required for correcting the octahedral tilt. The form of the Coulombic potential E_{c} is

$$E_{\mathrm{c}} = \frac{1}{4\pi\epsilon_0} \sum_{\beta} \sum_{\beta'} \left(\frac{q_\beta q'_\beta}{r_{\beta\beta'}} \right) \tag{2}$$

where ϵ_0 is the electrical permittivity of space, q_β is the fitting parameter which is close to the Mulliken charge of the atom of the type β, and $r_{\beta\beta'}$ is the bond length between two atoms of types β and β'. The form of the pairwise repulsive potential E_{r} is

$$E_{\mathrm{r}} = 8\epsilon \sum_{\beta} \sum_{\beta'} \left(\frac{B_{\beta\beta'}}{r_{\beta\beta'}} \right)^{12} \tag{3}$$

where ϵ is the energy unit of 1 eV, and $B_{\beta\beta'}$ is the fitting parameter. Brown *et al* produced the empirical inverse formula between the bond length and the bond valence as follows:

$$V_{\beta\beta'} = \left(\frac{r^0_{\beta\beta'}}{r_{\beta\beta'}} \right)^{C_{\beta\beta'}}, \tag{4}$$

 © 2008 IOP Publishing Ltd Printed in the UK

where $V_{\beta\beta'}$ is the bond valence and $r^0_{\beta\beta'}$ and $C_{\beta\beta'}$ are empirical parameters which are specific to the atom types to be bonded. For example, empirical $r^0_{\beta\beta'}$ and $C_{\beta\beta'}$ parameters are 1.806 Å and 5.2 for Ti–O and 2.044 Å and 5.5 for Pb–O [18]. Since the theoretical lattice constants ($a = 3.87$ Å and $c = 4.05$ Å) from the local density approximation are smaller than the experimental values ($a = 3.9$ Å and $c = 4.15$ Å), we corrected the $r^0_{\beta\beta'}$ parameter using the fact that the sum of bond valences should be the same as the atomic valence. The bond-valence potential E_b

$$E_\mathrm{b} = \sum_\beta S_\beta \left(\sum_{\beta'} V_{\beta\beta'} - V_\beta \right)^2 \tag{5}$$

favors each atom having bonding equal to its atomic valences V_β and provides a constraint, where V_β is the atomic valence and S_β is the fitting parameter. If all the ions in an ionic system have positions that give the preferred atomic valence, the potential E_b will be minimized. Thus, equation (5) keeps the sum of the bond strengths for each atom close to its desired atomic valence. The angle potential E_a is defined as

$$E_\mathrm{a} = k \sum_{i=1}^{N_\mathrm{oct}} \left(\theta^2_{i,x} + \theta^2_{i,y} + \theta^2_{i,z} \right) \tag{6}$$

where k is the angle potential parameter, N_oct is the number of oxygen octahedra, and $\theta_{i,k}$ is the angle of the opposite oxygen atoms relative to the reference axis along the k direction. All potential parameters used in this study are listed in table 1.

Using this model potential for $PbTiO_3$, we performed molecular dynamics simulations at constant temperatures below and above the experimental phase transition temperature T_c (765 K), controlling temperatures with the Nosé–Hoover thermostat as implemented in MOLDY[3]. In these simulations, the lattice constants were fixed to the experimental values while the z axis was set to the polar axis. The instantaneous local polarization $\mathbf{P_u}(t)$ is defined as:

$$\mathbf{P_u}(t) = \frac{1}{V_\mathrm{u}} \left(\frac{1}{8} \mathbf{Z}^*_\mathrm{Pb} \sum_{i=1}^{8} \mathbf{r}_{\mathrm{Pb},i}(t) + \mathbf{Z}^*_\mathrm{Ti} \mathbf{r}_\mathrm{Ti}(t) + \tfrac{1}{2} \sum_{i=1}^{6} \mathbf{Z}^*_{\mathrm{O},i} \mathbf{r}_{\mathrm{O},i}(t) \right), \tag{7}$$

where V_u is the volume of a unit cell, $\mathbf{Z}^*_\mathrm{Pb}$, $\mathbf{Z}^*_\mathrm{Ti}$, and $\mathbf{Z}^*_{\mathrm{O},i}$ are the Born effective charge tensors, and $\mathbf{r}_{\mathrm{Pb},i}$, $\mathbf{r}_\mathrm{Ti}$, and $\mathbf{r}_{\mathrm{O},i}$ are atomic positions of Pb, Ti, and O atoms in a unit cell at time t [19–21]. The polarization $\mathbf{P}$ was obtained from the time average of the sum of $\mathbf{P_u}(t)$ in a supercell divided by the number of unit cells. We also increased the number of unit cells in a supercell to remove the effect of periodic boundary conditions especially around the phase transition temperature. The profile of the polarization $\mathbf{P}$ at various temperatures between 300 and 800 K is shown in figure 1. At 300 K, the z component of $\mathbf{P}$ (P_z) is close to the experimental value (0.8 C m^{-2}), and the x and y components (P_x and P_y) are nearly zero with small fluctuation (figure 1(a)). As the temperature increases, the magnitude of the polarization $\mathbf{P}$ along the polar axis gradually decreases (figures 1(b) and (c)). At 700 K, the sign of P_z changes randomly with large fluctuation (figure 1(d)). At 800 K, the P_z component cannot be distinguished from the P_x and P_y components (figure 1(e)). Therefore, the computational ferroelectric phase transition temperature of $PbTiO_3$ corresponds to ∼700 K (figure 1(f)). The improved phase transition temperature of $PbTiO_3$ compared to reference [13] results from the additional reference structures with different c/a ratios.

[3] MOLDY is developed by Keith Refson, and it is a free software following the terms of the GNU General Public License.

Table 1. Optimized potential parameters of the bond-valence model potential function which were used in this study. The angle potential parameter k is 1.43 meV/(°)^2.

						$B_{\beta\beta'}$ (Å)		
β	V_β	$r^0_{\beta\mathrm{O}}$ (Å)	$C_{\beta\mathrm{O}}$	q_β (e)	S_β (eV)	Pb	Ti	O
Pb	2	1.969	5.5	1.419	0.013	—	2.224	1.686
Ti	4	1.804	5.2	1.036	0.223	2.224	—	1.201
O	2	—	—	−0.818	0.702	1.686	1.201	1.857

In order to examine the displacive and order–disorder characters of $PbTiO_3$, we analyzed the distances between one of the metal ions and its neighboring oxygen ions in the two extreme cases—temperatures below and above the computational phase transition temperature. Schematic diagrams of Pb–O and Ti–O bond lengths are shown in figure 2.

Below the phase transition temperature, three clearly separated peaks are observed for both Ti–O and Pb–O bonds. In figure 3(a), the histograms of Ti–O and Pb–O bond lengths are fitted to Gaussian functions. There are six nearest-neighbor oxygen ions for each Ti ion in a high-symmetry cubic structure. In a tetragonal structure, however, these oxygen ions do not have the same distances from the Ti ion. One of the two Ti–O bonds along the polar axis is the longest, another is the shortest, and the other four Ti–O bonds are in the middle. Therefore, the histogram of Ti–O bond lengths shows three peaks: a peak centered at 1.8 Å with the area of S, a peak centered at 2.4 Å with the area of S, and a peak centered at 2.0 Å with the area of $4S$ (figure 3(a)). Each Pb ion has twelve nearest-neighbor oxygen ions in a high-symmetry cubic structure. In a tetragonal structure, four of nearest-neighbor oxygen ions on a plane perpendicular to the polar axis form the shortest bonds to Pb, another four form intermediate bonds, and the other four form the longest bonds. Therefore, the histogram of Pb–O bond lengths will show three peaks with the same areas of $4S$: a peak centered at 2.5 Å, a peak centered at 3.3 Å, and a peak centered at 2.8 Å.

As the temperature increases, each peak becomes broader and broader until they become indistinguishable from one another (figure 3(d)). However, the shape of the merged peaks at the high temperature is not always symmetric. This asymmetry means the net displacement of each ion is not exactly zero, even above the phase transition temperature. In order to explain the symmetry of peaks, the analytic expression of the bond lengths might be helpful. The analytic expression

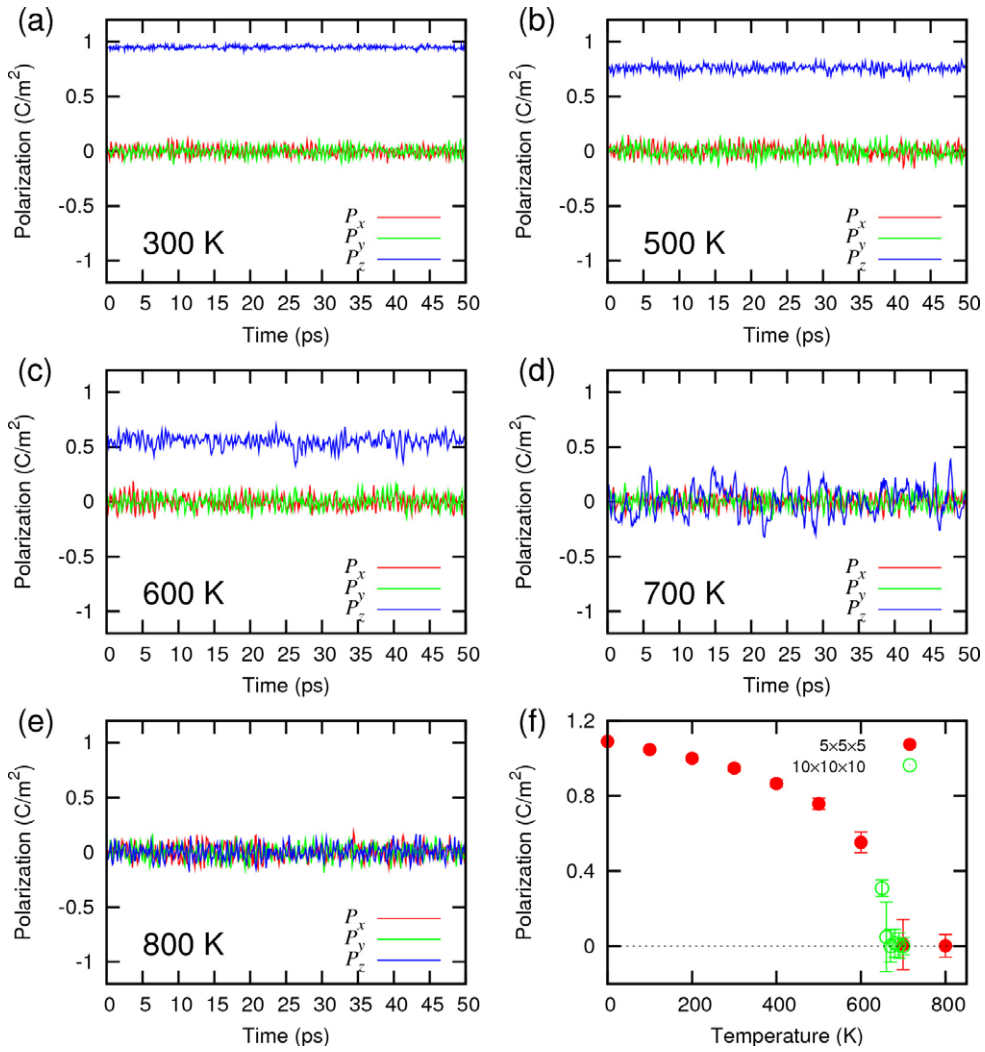

Figure 1. Temperature dependence of polarization of $PbTiO_3$. (a)–(e) Polarization profiles from molecular dynamics simulations during 100 ps below and above the phase transition temperature. (f) The phase transition behavior of $PbTiO_3$. The standard deviation of polarization is denoted with the vertical error bar at each point.

of the three bond lengths of Pb–O is

$$f_1 = \sqrt{\left(\frac{c}{2} - d_{\mathrm{Pb}}\right)^2 + \left(\frac{a}{2}\right)^2} \tag{8}$$

$$f_2 = \sqrt{\frac{a^2}{2} + d_{\mathrm{Pb}}^2} \tag{9}$$

$$f_3 = \sqrt{\left(\frac{c}{2} + d_{\mathrm{Pb}}\right)^2 + \left(\frac{a}{2}\right)^2}, \tag{10}$$

where d_{Pb} is the displacement of the Pb ion, and the analytic expression of the three bond lengths of Ti–O is

$$g_1 = \frac{c}{2} - d_{\mathrm{Ti}} \tag{11}$$

$$g_2 = \sqrt{\left(\frac{a}{2}\right)^2 + d_{\mathrm{Ti}}^2} \tag{12}$$

$$g_3 = \frac{c}{2} + d_{\mathrm{Ti}}, \tag{13}$$

where d_{Ti} is the displacement of the Ti ion. Since the Pb and Ti displacements are 0.4 and 0.3 Å at 100 K, the estimated distances among the centers of the three peaks for the Pb–O bonds are 0.14 and 0.30 Å, and the estimated distances among the centers of the three peaks for the Ti–O bonds are 0.32 and 0.48 Å. These analytic results show good agreement with the peaks in figure 3(a). At 800 K, the Pb and Ti displacements are about 0.1 and 0.2 Å, respectively. From the analytic expression of the Ti–O and Pb–O bonds, the distances among the Pb–O peaks are 0.07 Å, and the distances among the Ti–O peaks are 0.21 and 0.19 Å (figures 3(e) and (f)). The symmetric peak of Pb–O at 800 K can be explained using this analytic expressio of the bond length.

When the histogram of the Ti displacement below T_c is compared with the histogram of the Ti displacement above T_c, the order–disorder character of $PbTiO_3$ becomes clear (figure 4). The largest one among x, y, and z components of the displacement vectors of Ti and Pb ions is chosen to make these histograms. Below T_c, the distribution of each ion has a single peak with the same sign of displacements as shown in

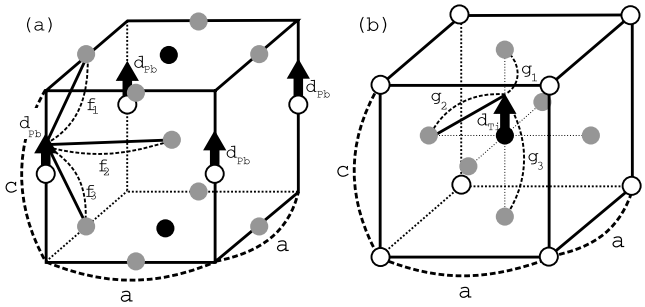

Figure 2. Diagrams of (a) Pb–O and (b) Ti–O bonds in a unit cell of $PbTiO_3$. Black, white, and gray circles denote Ti, Pb, and O, respectively. Arrows demonstrate the displacements of Pb and Ti ions.

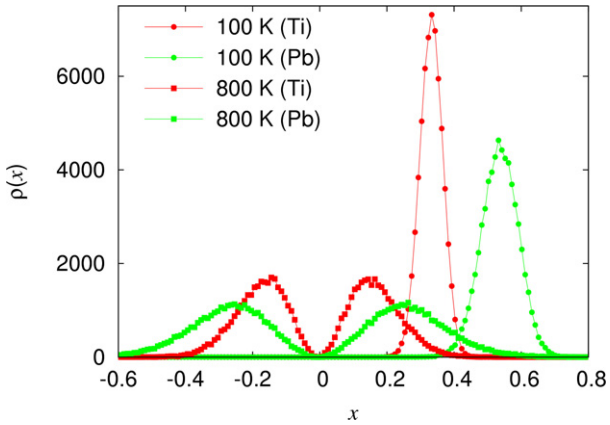

Figure 4. Histograms of Ti and Pb displacements of $PbTiO_3$.

figure 4 with black (red in the electronic version) solid circles. If $PbTiO_3$ had only the displacive character, the displacement distribution above T_c should be a single peak. Black squares (blue solid circles in the electronic version) in figure 4 show that the distribution of the Ti displacement has symmetric double peaks, which confirms that there is an order–disorder characteristic for $PbTiO_3$ in the paraelectric phase. The same behavior was shown for the Pb displacement in figure 4.

In conclusion, we studied the displacive and order–disorder characters of $PbTiO_3$ with the classical atomic model which has been developed under the inverse relation between the bond length and the bond valence. From the additional reference structures with different c/a ratios, we obtained the improved phase transition temperature of 700 K and the spontaneous polarization of 0.9 C m^{-2} at 300 K which is close to the experimental value.

To examine the displacive and order–disorder characters of $PbTiO_3$, we analyzed the histograms of Ti–O and Pb–O bond lengths which have three clearly separated peaks as Gaussian forms below the phase transition temperature. Also, the displacement distributions of Ti and Pb have a single peak below the phase transition temperature, indicating the displacive character of $PbTiO_3$. Such a displacive character can be found from the decrease of the polarization as the temperature increases. In the paraelectric phase, however, the displacement distributions of Ti and Pb show symmetric double peaks, which reveals an order–disorder characteristic of $PbTiO_3$.

Acknowledgments

This work was supported by the Brain Korea 21 Project in 2006, by the US Office of Naval Research, under grants N00014-00-1-0372 and N00014-01-1-0365, and by the US NSF MRSEC Program, Grant DMR05-20020. Computational support was provided by a Challenge Grant from the HPCMO of the US Department of Defense.

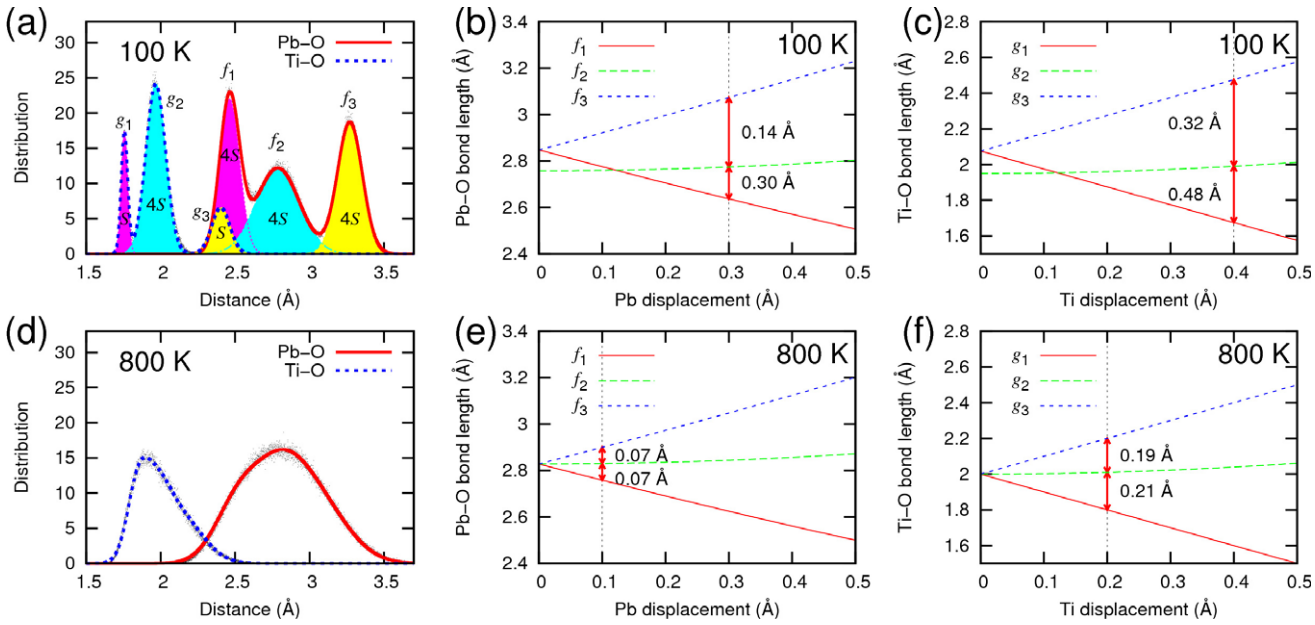

Figure 3. Smeared histograms of the Ti and Pb displacement at (a) 100 K and (d) 800 K. The centers of peaks can be analytically shown using the Pb–O and Ti–O bond lengths as functions of Ti and Pb displacements, respectively at 100 K (b) and (c) and 800 K (e) and (f).

References

[1] Lines M E and Glass A M 1977 *Principles and Applications of Ferroelectrics and Related Materials* (Oxford: Clarendon)
[2] Miller R C and Weinreich G 1960 *Phys. Rev.* **117** 1460
[3] Tybell T, Paruch P, Giamarchi T and Triscone J M 2002 *Phys. Rev. Lett.* **89** 097601
[4] Comes R, Lambert M and Guinier A 1968 *Solid State Commun.* **6** 715
[5] Dougherty T P, Wiederrecht G P, Nelson K A, Garrett M H, Jensen H P and Warde C 1992 *Science* **258** 770
[6] Krakauer H, Yu R, Wang C, Rabe K M and Waghmare U V 1999 *J. Phys.: Condens. Matter* **11** 3779
[7] Fontana M D, Idrissi H, Kugel G E and Wojcik K 1991 *J. Phys.: Condens. Matter* **3** 8695
[8] Nelmes R J, Piltz R O, Kuhs W F, Tun Z and Restori R 1990 *Ferroelectrics* **108** 165
[9] Kiat J, Uesu Y, Dkhil B, Matsuda M, Malibert C and Calvarin G 2002 *Phys. Rev.* B **65** 064106
[10] Cohen R E 1992 *Nature* **358** 136
[11] Sepliarsky M, Stachiotti M G and Migoni R 1995 *Phys. Rev.* B **52** 4044
[12] Grinberg I, Cooper V R and Rappe A M 2002 *Nature* **419** 909
[13] Shin Y H, Cooper V R, Grinberg I and Rappe A M 2005 *Phys. Rev.* B **71** 054104
[14] Sepliarsky M, Stachiotti M G and Migoni R L 2006 *Phys. Rev. Lett.* **96** 137603
[15] Shin Y H, Grinberg I, Chen I W and Rappe A M 2007 *Nature* **449** 881
[16] Zhong W, Vanderbilt D and Rabe M K 1994 *Phys. Rev. Lett.* **73** 1861
[17] Marques M I 2005 *Phys. Rev.* B **71** 174116
[18] Brown I D and Wu K K 1976 *Acta Crystallogr.* B **32** 1957
[19] King-Smith R D and Vanderbilt D 1993 *Phys. Rev.* B **47** 1651
[20] Resta R 1994 *Rev. Mod. Phys.* **66** 899
[21] Ghosez P, Cockayne E, Waghmare U V and Rabe K M 1999 *Phys. Rev.* B **60** 836